Z. Phys. A 356, 293–297 (1996)

ZEITSCHRIFT
FÜR PHYSIK A

$^7Be(p,\ \gamma)^8B$ cross section from indirect breakup experiments

C.A. Bertulani⋆

Gesellschaft für Schwerionenforschung, KPII, Planckstrasse 1, D-64291 Darmstadt, Germany

Received: 24 May 1996 / Revised version: 20 July 1996
Communicated by W. Weise

Abstract. The amplification of the E2 and M1 electromagnetic transitions in the radiative capture reaction $^7Be(p,\gamma)^8B$ is investigated. This amplification occurs in Coulomb dissociation experiments. Interference between the excitation amplitudes of E1, E2 and M1 multipolarities leads to anisotropy effects in the angular distribution of the fragments. Dynamical coupling which could affect the direct correspondence between the Coulomb breakup and the radiative capture cross sections are studied by means of a coupled-channels approach.

PACS: 25.60.+v;25.70.De;25.70.Mn

The Coulomb dissociation has become an important tool [1], to obtain the radiative capture cross sections of astrophysical relevance by inverse kinematics. For example, in a recent experiment by Motobayashi et al. [2] valuable information on the reaction $^7Be(p,\ \gamma)^8B$, important for the flux of high energy neutrinos from the Sun [3], was obtained. The experiment generated much debate in the literature concerning the multipolarity content of the measured spectra [4, 5, 6, 7, 8]. It was observed that, although E2 transitions are not relevant for the capture cross section at low energies, they are amplified in Coulomb dissociation experiments [4]. Esbensen and Bertsch [7] have recently studied the E2 contribution to the breakup and suggested a way to deduce its magnitude by looking at the intrinsic angular distribution of the fragments. However, the M1 transitions to the $J = 1^+$ continuum state were not included in the calculation. The M1 transitions are dominant at the region close to the $J = 1^+$ state (E_r = 0.63 MeV). A good part of the relative energy between the fragments accessed by Coulomb dissociation experiments includes this energy region. As shown in [6], M1 transitions are very important for the experiment planned at the GSI/Darmstadt facility (at E_{Lab} = 250 MeV.A) [9]. In this article it is shown that the M1 transitions to the $J = 1^+$ state affect significantly the cross sections and angular distribution of the fragments. A study of the effects of higher-order processes is also investigated with a coupled-channels calculation.

We use for ^8B a similar model as in [10], assuming that the 2^+ ground state can be described as a $p3/2$ proton coupled to the $3/2^-$ ground state of the ^7Be core. The spectroscopic factor for this configuration was taken as unity. The single particle states ϕ^J_{Elj} are found by solving the Schrödinger equation with spin-orbit term and matching to asymptotic Coulomb waves. The parameters of the potentials are given in Table 1. The width of the $J = 1^+$ and $J = 3^+$ states are found by using the definition $\Gamma_r = 2(d\delta/dE)^{-1}_{E=E_r}$, where $\delta(E)$ is the phase shift of the partial wave solution with energy E. The resonance energy, E_r, is defined as the energy where the derivative is largest. The total wavefunction is constructed by coupling the single-particle states with the spin of the ^7Be core, $I_c = 3/2^-$. To compute the S-factors for the capture process $b + x \rightarrow a$ we have used the first-order perturbation theory and the matrix elements for electric multipole states (we couple angular momentum as $\mathbf{l} + \mathbf{s} = \mathbf{j}$, and $\mathbf{j} + \mathbf{I_c} = \mathbf{J}$) given by

$$
\begin{aligned}
&< J_2M_2|\mathscr{M}(E\lambda\mu)|J_1M_1 > \\
&= \frac{e_\lambda}{\sqrt{4\pi}}(-1)^{j_1+I_c+J_1+l_1+l_2+\lambda}\ \frac{\hat{\lambda}\hat{j}_1\hat{J}_1}{\hat{j}_2} \\
&\times (J_1M_1\lambda\mu|J_2M_2)\ (j_1\lambda\frac{1}{2}0|j_2\frac{1}{2}) \\
&\times \left\{ \begin{array}{ccc} j_2 & J_2 & I_c \\ J_1 & j_1 & \lambda \end{array} \right\} \mathscr{O}(1 \rightarrow 2;\ \lambda) \qquad (1)
\end{aligned}
$$

where $\mathscr{O}(1 \rightarrow 2;\ \lambda) = \int \phi^{J_2}_{E_2l_2j_2}(r)\ \phi^{J_1}_{E_1l_1j_1}(r)\ r^\lambda dr$ is the overlap integral, $\hat{k} \equiv \sqrt{2k+1}$, and $e_\lambda = Z_be(-A_x/A_a)^\lambda + Z_xe(A_b/A_a)^\lambda$ is the effective electric charge. The M1 transition matrix elements are

$$
\begin{aligned}
&< J_2M_2|\mathscr{M}(M1\mu)|J_1M_1 > \\
&= \mu_N\ (-1)^{j_1+I_c+J_1+1}\ \frac{\hat{J}_1}{\hat{l}_1}\ (J_1M_1 1\mu|J_2M_2)\ \left\{ \begin{array}{ccc} j_2 & J_2 & I_c \\ J_1 & j_1 & 1 \end{array} \right\} \\
&\times \Bigg\{ e_M\ \Bigg[2\frac{\tilde{j}_1}{\hat{l}_1}\ \left(l_1\delta_{j_1,l_2+\frac{1}{2}} + (l_2+1)\delta_{j_1,l_2-\frac{1}{2}} \right) \\
&+(-1)^{l_1+\frac{1}{2}-j_2}\ \frac{\hat{j}_1}{\hat{2}}\delta_{j_1,l_1\pm\frac{1}{2}}\delta_{j_2,l_2\mp\frac{1}{2}} \Bigg]
\end{aligned}
$$

⋆ *Permanent address:* Instituto de Física, Universidade Federal do Rio de Janeiro 21945-970 Rio de Janeiro, RJ, Brazil (e-mail: bertu@if.ufrj.br)

Table 1. Parameters of the potential $V(r) = V_0\left[1 - F_{s.o.}(\mathbf{l}.\sigma)\ \frac{r_0}{r}\ \frac{d}{dr}\right]$ $[1+\exp((r-R)/a)]^{-1}$ used in the calculation of the proton+^7Be wavefunction. The remaining parameters are a = 0.52 fm, r_0 = 1.25 fm, R = 2.391 fm, and $F_{s.o.}$ = 0.351 fm. The width of the $J = 1^+$ and $J = 3^+$ are given in the last column. The Coulomb potential is that of a uniform charge distribution with the radius R

$(l,$j$)$	$E\ [MeV]$	$V_0\ [MeV]$	$\Gamma\ [MeV]$
Ground state	–0.14	–44.658	
$s1/2,\ d3/2,\ d5/2$	$0-3$	–42.48	
$p1/2,\ p3/2,\ f5/2,\ f7/2$	$0-3$	–42.48	
$p3/2$ ($J = 1^+$)	0.63	–42.48	0.064
$p3/2$ ($J = 3^+$)	2.17	–36.05	1.504

$$+g_p\ \left[(-1)^{l_1+\frac{1}{2}-j_1}\ \frac{\tilde{j}_1}{\hat{l}_1}\delta_{j_1,j_2}\right.$$
$$\left.-(-1)^{l_1+\frac{1}{2}-j_2}\ \frac{\hat{j}_1}{\hat{2}\hat{l}_1}\ \delta_{j_1,l_2\pm\frac{1}{2}}\delta_{j_2,l_2\mp\frac{1}{2}}\right]\Big\}\mathscr{O}(1\to 2;\ \lambda=0)$$
$$+\mu_c\ (-1)^{I_c+j_1+J_2+1}\ (J_1M_1 1\mu|J_2M_2)\ \hat{J}_1\hat{J}_2\hat{I}_c\tilde{I}_c$$
$$\times\left\{\begin{array}{ccc} I_c & J_2 & j_1 \\ J_1 & I_c & 1\end{array}\right\}\mathscr{O}(1\to 2;\ \lambda=0) \qquad (2)$$

where $e_M = m_{bx}(Z_x/m_x + Z_b/m_b)$, $\mu_N = e\hbar/2m_pc^2$, and $\tilde{k} = \sqrt{k(k+1)}$. Following Robertson [10], we use $\mu_c = -1.7\ \mu_N$ for the magnetic moment of ^7Be.

Due to the very low binding, the bound state wave function is very diluted and to achieve a good precision we need to calculate the overlap integrals $\mathscr{O}(1 \to 2)$ up to 200 fm. We have considered s, p, d an f continuum states, as displayed in Table 1. The calculated S-factors as a function of the $p-^7Be$ relative energy are given in Fig. 1a, together with the experimental data. The contribution of the M1 transitions to the $J = 1^+$ resonance strongly influences the spectrum in the energy interval between 0.5 and 0.8 MeV [8]. Outside this energy interval the spectrum is completely dominated by the E1 transitions (to the s and d waves) which is about 3 orders of magnitude larger than the E2 transitions (to the p and f waves). This model predicts an S-factor at E=0 equal to 17.7 eV.b. The data seem to favor a larger value of the S-factor. However, the data of Motobayashi et al. [2] imply a lower value of the S-factor (S_{E1} = 16.7 ± 3.2 eV.barn) compared to the other experiments, and is in rough agreement with the result of this simple potential model. However, some care is needed before drawing too strong conclusions about these results. It is well known that the potential model does not provide a precise description of the resonant states of ^8B [11].

We use the potential model as input to calculate the Coulomb excitation cross sections, following the description presented in [6]. In Fig. 1b we show the breakup cross sections folded with the detector efficiency. We see that the E2 contribution is enormously amplified by the time-dependent Coulomb field of the target, as was earlier pointed out by Langanke and Shoppa [4]. Including the M1 and E2 contributions, a good agreement with the data is found. This is rather surprising, since the same radiative capture model can not describe the data set of Motobayashi et al. [2], as seen in Fig. 1a. For example, the S-factor data point at 0.6 MeV would yield a negligible Coulomb breakup cross section, not compatible with the data set of Fig. 1b. A recent explanation for this was given by Esbensen and Bertsch [7] who claim

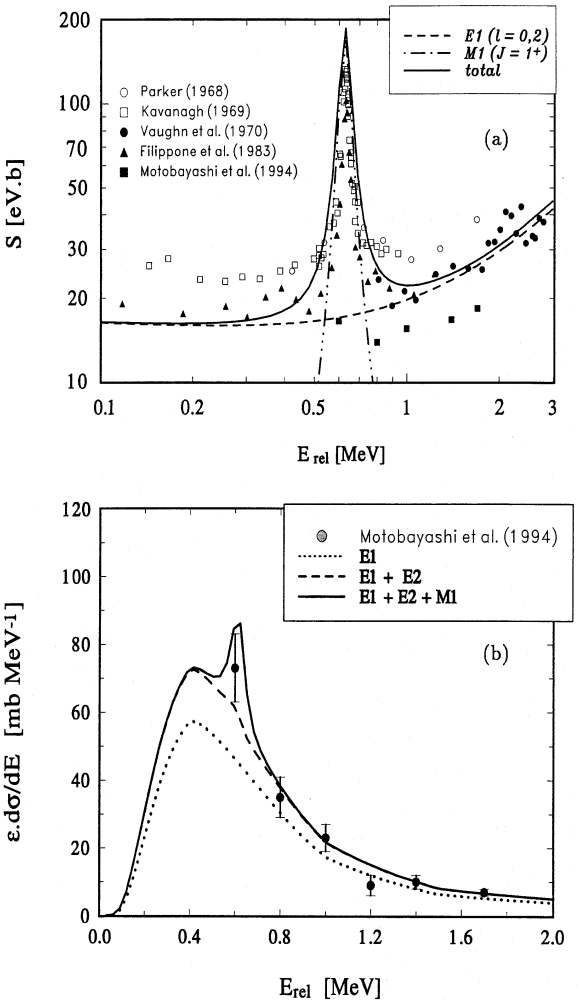

Fig. 1. a S-factors compiled from several experiments and compared to the potential model calculation. The dot-dashed line is the contribution from M1 transitions to the $J = 1^+$ state at 0.63 MeV. The dashed line is the contribution of E1 transitions to the s and d waves. The solid line includes both E1 and M1 transitions. The E2 transitions are not shown because they are too small. **b** Coulomb dissociation spectrum for the $^8B + Pb \longrightarrow p + ^7Be + Pb$ reaction at E_{Lab} = 46.5 A.MeV. The data are from [2]. The contribution of each multipolarity transition is shown

that the interference between E1 and E2 transitions due to higher order continuum-continuum coupling is responsible for the quenching of E2 direct transitions. Later on this paper we shall investigate this effect with a coupled-channels calculation.

The inclusion of the M1 transitions is very important for the analysis of the experimental data, and have not been considered in previous analysis [2, 4, 7]. While the magnitude of the E2 transitions in the radiative capture cross section is very model dependent and controversial, the M1 transitions to the $J = 1^+$ are well known experimentally and can be safely used as a guide to the planned Coulomb breakup experiments. In fact, at the energies of 250 MeV/nucleon the Coulomb breakup is dominated by M1 transitions to the the $J = 1^+$ state for $0.5 < E < 0.8$ MeV, as was shown in [6]. Measurements outside this region would be more suitable to separate the E1 and E2 contributions.

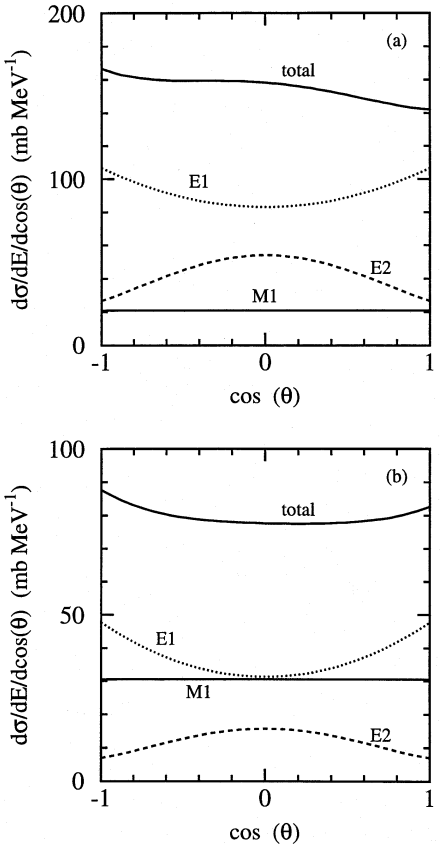

Fig. 2. a Angular distribution of the angle θ between the proton and the beam direction in the $^8B + Pb \longrightarrow p +^7 Be + Pb$ reaction at E_{Lab} = 46.5 A.MeV. A minimum impact parameter b = 15 fm was used in the calculations. The contribution of each multipolarity is shown separately. **b** Same as in **a**, but for E_{Lab} = 250 A.MeV

In [7] the angular distribution between the fragments in the Coulomb breakup of ^8B on lead targets was studied. As an example, the angular distribution was calculated for the relative energy of E_{rel} = 0.6 MeV. We have included transitions to the $J = 1^+,\ 3^+$ states for the same case. The results are shown in Fig. 2 for ^8B projectiles at (a) 46.5 A.MeV and (b) 250 A.MeV, respectively. A minimum impact parameter of 15 fm was used in the calculations. In agreement with [7], we find that the interference between the E1 and E2 transitions leads to an anisotropy in the angular distribution at 46.5 A.MeV. However, we see in Fig. 2b that this anisotropy disappears at the bombarding energy of 250 A.MeV. Note that the influence of M1 transitions are much stronger at 250 A.MeV. It should be noted that it will be very hard to extract the E2 contributions by measuring the interference in the angular distribution of the fragments. Moreover, the interference pattern in the angular distribution function is strongly dependent on the magnitude and on the phases of the matrix elements. Since these matrix elements are dependent on the ^8B model one is using, there is no guarantee that the patterns shown in Fig. 2 present a reliable guide to the experiments.

We have also analysed the effect of reacceleration of the fragments in the Coulomb field of the target, after the breakup occurs. This effect has been studied by many authors [5, 6, 7]. More recently, it has been studied in [7] using the single particle model for ^8B [10]. The calculation method in [7] is based on the solution of the time-dependent Schrödinger equation, starting with the ground state wavefunction, and obtaining the final wavefunction by repeated application of an unitary operator. A drawback of the method is that during the time integration the nuclear potential parameters are kept fixed with values chosen to reproduce the ground state energy. Since this set of parameters does not reproduce simultaneously the position of the resonant states, the transitions to the $J = 1^+$ state at 0.63 MeV are not properly accounted for. The spin-orbit interaction has also been neglected in the dynamical calculations. On the other hand, such problems can avoided straightforwardly by means of a coupled-channels calculation. One needs the matrix elements as given by equations (1) and (2), for ground-state to continuum and continuum to continuum transitions. All continuum states, including resonant states, with correct energies can be included.

A drawback of the coupled-channels method is that the continuum-continuum transitions lead to matrix elements $< \phi_2|r^\lambda|\phi_1 >$ which diverge due to the non-localized behaviour of the wavefunctions. The localization may be achieved by requiring appropriate boundary conditions like the normalization of the continuum states in a large box. However, this method requires an excessive number of these quasi-bound states to account for a rapidly varying resonance imbedded in the continuum. Moreover, due to the small binding energy of the bound state, a very large box of several hundreds of fermi is needed. This leads to convergence problems in numerical calculations. A better procedure is to discretize the continuum by constructing wave packets. This procedure has been used, e.g., in [12] to study the effects of reacceleration in the Coulomb breakup of the halo nucleus ^{11}Li.

From the single particle wave functions ϕ_{Ejl} we construct wave packets according to

$$\phi_{E_i jl}(r) = \frac{1}{\sqrt{\Delta E}} \int_{E_i-\Delta E/2}^{E_i+\Delta E/2} \phi_{Ejl}(r) dE \qquad (3)$$

We use energy intervals of 50 keV for $E_{rel} < 0.5$ MeV and $0.7\ MeV < E_{rel} < 3\ MeV$, and 10 keV for the energy interval 0.5 MeV $< E_{rel} <$ 0.7 MeV, respectively. Since the continuum wavefunctions have an asymptotic behaviour of a sine function, i.e., $\phi \sim \sin(kr + \delta_k)$, the discretization procedure yields asymptotic functions with the approximate behaviour $\phi^{(i)} \sim \sin(k_i r + \delta_{k_i})/r$. This ensures the convergence of the matrix elements, at least for E1 and M1 transitions. As for E2 transitions, a good convergence of the matrix elements was not obtained and they were not taken into account. However, as one sees from Fig. 2b, Coulomb dissociation favors E1 transitions, and we think that the E1 and M1 continuum-continuum transitions can account for the most part of the dynamical effects. Therefore, in the calculations presented here there are two kinds of continuum-continuum coupling: (a) E1 transitions between the $(s,\ d)$ and the $(p,\ f)$ non-resonant states and (b) M1 transitions between the (p, f) non-resonant and the $p3/2^{J=1^+}$ resonant state.

In Fig. 3a we show the transition strength function $d^2B(E1)/dk_1\ dk_2$ for continuum-continuum E1 transitions

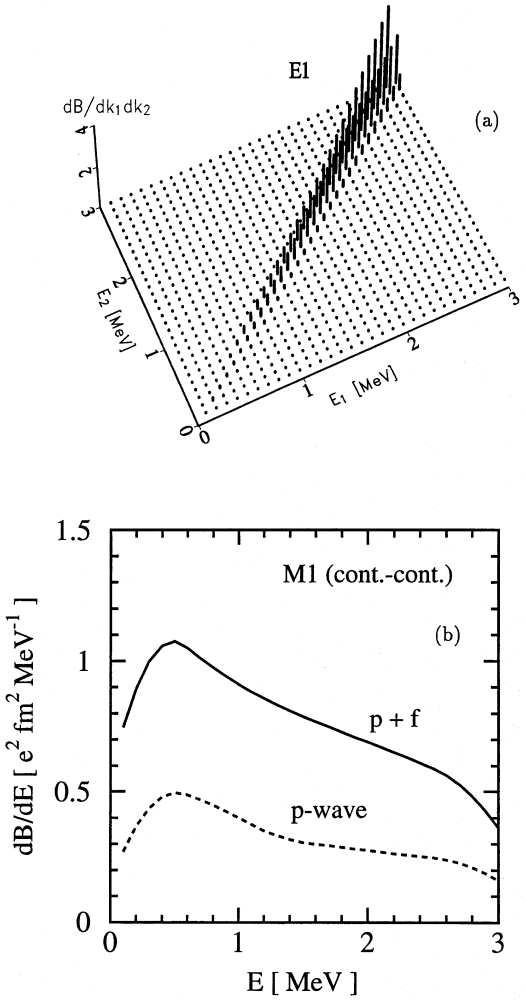

Fig. 3. a Continuum-continuum strength function, $dB(E1; E_1 \rightarrow E_2)/dk_1dk_2 = \sum_{\mathbf{J_2}} | < J_2||\mathscr{M}(E1)||J_1 > |^2/(2J_1 + 1)$, in units of $10^5\ e^2fm^5$, as a function of $E_i = \hbar^2k_i^2/2\mu_{bx}$. **b** M1 continuum-continuum strength function for transitions from the $J = 1^+$ state to other continuum states. The strength was integrated over the width of the resonant $J = 1^+$ state

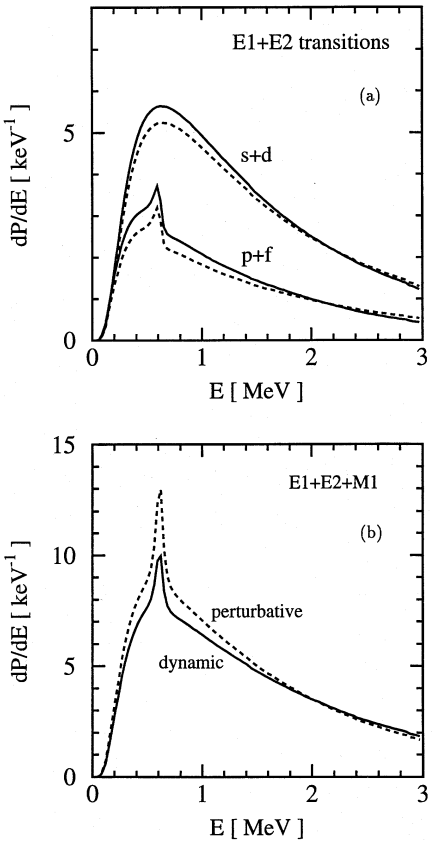

Fig. 4. a Differential probability dP/dE for first-order transitions (solid lines) from the ground state to the s and d (E1 transitions) and to the p and f states (E2 transitions) in ^8B projectiles incident on lead targets at 46.5 A.MeV with impact parameter b = 15 fm. The dashed lines include the E1 continuum-continuum coupling between the $(s,\ d)$ and the $(p,\ f)$ states. **b** Differential probability dP/dE for E1+E2+M1 first-order transitions (dashed line) from the ground state. The solid line is from coupled-channels dynamical calculations, which include not only the E1 transitions (as in **a**), but also the M1 continuum-continuum coupling between the $(p3/2^{1^+})$ and the $(p,\ f)$ waves

$(1 \rightarrow 2)$, as a function of the continuum energies $E_i = \hbar^2k_i^2/2\mu_{bx}$. The transitions are stronger close to the diagonal, $(E_1 \sim E_2)$, increasing with the relative energy of the fragments. This result is consistent with the analytical formulas obtained in [12] (eq. 3.12), where plane waves were used to calculate the continuum-continuum matrix elements. In Fig. 3b we show the strength function $dB(M1)/dE$, for M1 transitions from the $J = 1^+$ resonance state to the $p1/2$, $f5/2$ and $f7/2$ continuum states. The strength function was integrated over the energy interval where the resonance makes an appreciable contribution $(0.5 - 0.7$ MeV). The M1 transitions from the $J = 1^+$ state to neighbouring continuum states is about an order of magnitude larger than E1 transitions from the ground state to the continuum. This means that M1 transitions can affect the energy spectrum around $E = 0.5 - 0.8$ MeV appreciably more than E1 and E2 continuum-continuum transitions. However, these are higher-order processes, which can only occur after the first step excitation to the continuum states is taken. Since first step transitions induced in Coulomb dissociation have small amplitudes, it is expected that higher-order effects are only relevant for the closest collisions, for which the Coulomb excitation amplitudes are larger.

We performed a coupled-channels calculation using the time-dependent E1, E2, and M1 Coulomb fields of the target, including relativistic effects. The projectile is assumed to follow a straight-line trajectory with velocity v and impact parameter b. The coupled channels calculation is performed in the time interval $-10\ b/\gamma v < t < 10\ b/\gamma v$, and in steps $\Delta t = 0.01(b/\gamma v)$, where γ is the Lorentz factor. We note that $b/\gamma v$ is the time interval during which the Coulomb field of the target is strongest in the frame of reference of the projectile. The results for the differential probabilities dP/dE, where E is the relative energy between the proton and the ^7Be, are shown in the Fig. 4, for an impact parameter b = 15 fm. In Fig. 4a the M1 continuum-continuum transitions were switched-off. The solid lines represent E1 and E2 ground-state-to-continuum (s, d) and (p, f) waves, respectively. The dashed-lines include E1 continuum-continuum (as well as continuum-to-ground state) transitions. The peak at $E \sim 0.6$ MeV in the E2 transition probability is due to the $J = 1^+$ state. The continuum-continuum coupling reduces the tran-

sition probabilities at lower energies and shifts them slightly to higher energies. This effect is consistent with the results obtained in [6, 7]. However, the magnitude of the effect is smaller than that observed in [7]. This could be due to the neglect in our calculation of the E2 continuum-continuum transitions between the s and d and between the p and f states in the continuum, respectively. In Fig. 4b we show the final effect when M1 transitions are included (dashed line), compared to first order perturbation theory (s, d, p and f waves included). We see that the spectrum is influenced by dynamical effects in the energy interval close to the $J = 1^+$ state. The resonance peak is appreciably reduced. This is mainly due to the coupling of the $J = 1^+$ state to neighbouring p and f states, which reduces the occupation probability of the $J = 1^+$ state.

We conclude that the spectra of the relative energy between the proton and the ^7Be fragments is strongly influenced by M1 transitions involving the $J = 1^+$ state in ^8B. The potential model results do not agree with the experimental data for the S-factor from the experiment of [2]. However, the Coulomb dissociation spectrum, based on the same model, agrees very well with the Coulomb dissociation data from the same experiment. This situation is rather unsatisfactory and deserves further experimental investigation. We have also seen that the M1 (and E2) transitions interfere with the E1 transitions in the angular distributtion between the fragments. This could be useful to disentangle the contribution of different multipolarities to the dissociation process, and supports the results obtained in [7], where only E1 and E2 transitions were considered. However, we deduce that at higher energies ($E \sim 200$ A.MeV) the E1, E2 and M1 interference effects do not induce to noticeable asymmetries in the angular distributions.

The effects of reacceleration, i.e., continuum-continuum coupling, have been studied by means of a coupled-channels calculation. It was found that higher-order transitions does not modify the spectrum appreciably. In fact, the influence of higher order transitions decreases dramatically with the increasing impact parameter, as shown in previous studies [6]. Due to small energy (0.14 MeV) required to dissociate ^8B, the main contribution to the total cross section comes from collisions at large impact parameters for which the reacceleration effect is negligible. Thus, while the effect could be seen in differential cross sections corresponding to large scattering angles, it does not show up in total (impact parameter integrated) cross sections. Moreover, as shown in [6], higher-order effects tend to decrease as the bombarding energy increases. This favors experiments at higher bombarding energies, as the one proposed at the GSI for 250 A.MeV [9].

At present, the best way to separate the undesired E2 contributions in the Coulomb dissociation spectrum is to look at the angular distribution of the center-of-mass scattering of the ^8B by the inclusive measurement of the proton and the ^7Be fragment. As shown in [6] the E2 transitions contribute to large angle scattering, while E1 contributions are concentrated at much smaller scattering angles. Thus, the E1 contribution can be separated from E2 ones by a simple integration over the scattering distribution up to a maximum value where E2 transitions become large.

The author acknowledges partial support by the Fundação Universitária José Bonifácio and by the Conselho Nacional de Desenvolvimento Científico e Tecnológico (Brazil).

References

1. G. Baur, C.A. Bertulani, H. Rebel: Nucl. Phys. **A458** (1986) 188
2. T. Motobayashi et al.: Phys. Rev. Lett. **73** (1994) 2680
3. J.N. Bahcall: Neutrino Astrophysics (Cambridge University Press, New York, 1989)
4. K. Langanke, T.D. Shoppa: Phys. Rev. **49** (1994) 1771; M. Gai, C.A. Bertulani: Phys. Rev. C **52** (1995) 1706
5. S. Typel, G. Baur: Phys. Rev. **C50** (1994) 2104
6. C.A. Bertulani: Phys. Rev. **C49** (1994) 2688; Nucl. Phys. **A587** (1995) 318
7. H. Esbensen, G.F. Bertsch: Phys. Lett. **B359** (1995) 13; Nucl. Phys. **A**, in press
8. R. Shyam, I.J. Thompson, A.K. Dutt-Mazumder: Phys. Lett. **B**, in press
9. K. Suemmerer at al.: GSI/Darmstadt experiment proposal, accepted.
10. R.G. H. Robertson: Phys. Rev. **C7** (1973) 543
11. F.C. Barker: Aust. J. Phys. **33** (1980) 177
12. C.A. Bertulani, F. Canto: Nucl. Phys. **A539** (1992) 163